

Robot Interaction Force Estimation Using an Adaptive Sliding Mode Observer

Yanjun WANG^{1,2}, Yunfei ZHANG^{1,2}, Shujun GAO^{1,2}, Clarence W. DE SILVA²

(1.ViWiSTAR Technologies Ltd., Vancouver, Canada, V6T 1Z4;

2.Dept. of Mechanical Engineering, University of British Columbia, Vancouver, Canada, V6T 1Z4)

Abstract: In constrained motion control of a robot, the interaction force is an important variable, which directly describes the state of interaction. It is required in a number of algorithms for interaction control. Desirably, the interaction force has to be measured by force sensors. However, there are inherent limitations with force sensors, such as the cost, sensing noise, limited bandwidth, and the difficulty of physical location at the required place, which is dynamic. In the present paper, the interaction force is estimated by using high order sliding mode observers. An adaptive version of a high order sliding mode observer is developed to robustly reconstruct the interaction force. Experimental results are given to show the effectiveness of the developed algorithms.

Key words: Constrained Motion, Robot Manipulator, Adaptive Estimation, Sliding Mode Observer, Dynamic Identification.

1 Introduction

Interaction control is an important problem in practice^[1,2] for a constrained robot manipulator even though it is not applicable in free space motion control. During the interaction phase, the interaction force provides rather direct and representative information about the state of interaction. However, interaction force information is not conveniently and accurately available through direct sensing. To sense the interaction force between a robot manipulator and its interacting objects, a force sensor has to be mounted at the location of interaction, which is moving with limited access and may also be delicate. For these reasons, the force measurement is usually done at the wrist of the robot hand. The force that is sensed in this manner has to be calibrated and filtered before it can be used in an interaction controller. The resulting information may still be inaccurate because what is sensed is the internal force at the wrist while what is needed is the real interaction force between the robot end-effector and the interacting object^[3-5]. As pointed out^[6,7], the application of a force sensor may introduce some unavoidable problems, such as sensing noise, limited bandwidth,

and self-varying properties due to temperature change, in addition to the previously mentioned difficulties. Reconstruction of the interaction force through estimation algorithms instead of direct measuring is preferable in this context. The interaction force was considered as an external disturbance and estimated by using a disturbance observer where the estimation error converged to zero, asymptotically^[8,9]. The estimated interaction force information was then applied in a force control algorithm. It was shown analytically and experimentally that the algorithm could reconstruct the interaction force and guarantee the stability of the combined observer-controller system. Also, the bandwidth of the system increased as a result. Since the interaction force estimation only converged asymptotically, true real-time information of the force was not realized. The robot manipulator was commanded to follow exactly the same trajectories in both free motion and constrained motion^[10]. The difference between the joint torques in these two cases was taken to represent the external interaction force. The interaction force was reconstructed in this manner. However, this approach has limitations not only in its theoretical analysis, but also in practical implementation. In particular, controlling a robot to

follow exactly the same trajectories in both free and constrained motions is a major challenge.

The past work that is mentioned here also has the common limitation that an precise dynamic model of the robot manipulator is assumed, even though this is not quite realistic. The dynamic model was identified through least-squares estimation of the dynamic parameters just before interaction^[11]. The identified dynamic model was used for the external force estimation. The torque difference due to the external interaction force was calculated by comparing the joint torque predicted by the identified dynamic model and the actual actuating torques at each joint. The effectiveness of the proposed algorithm was tested using an one-degree-of-freedom manipulator through numerical simulation. A limitation of this method is that the velocity is obtained by directly differentiating the position measurement with respect to time. This may be acceptable in numerical simulations, but in physical implementations, measured joint position contains noise^[12]. Such noise will be amplified in the velocity that is obtained by differentiation and the result may be unacceptable in controller implementations. Another limitation of that approach is the assumption that some dynamic parameters such as the coefficient of friction are constant during both free and constrained motions. This assumption can be unrealistic since, for example, past work has indicated that the coefficient friction is time-varying and uncertain^[13,14].

Since the joint velocity information is required in interaction control algorithms, preferably, it should be estimated^[15-17]. Simultaneous estimation of joint velocity and external force is particularly desirable for interaction control algorithms. Sliding mode observer, which is a robust observation algorithm, finds its application in this context. A second-order sliding mode observers was applied to simultaneously estimate the velocity and the external interaction force^[18,19]. Experimental results were given to show the effectiveness of the algorithm. An accurate dynamic model of the robot manipulator was assumed

in their work. Also, the interaction force was estimated based on the concept of equivalent output feedback^[20]. A low-pass filter was applied to obtain the interaction force signal. Due to the use of a low-pass filter, a compromise had to be made between the smoothness and the time lag of the estimated interaction force.

The present work is inspired by the early work^[19,21-23], which provides more accurate estimates of the interaction force and velocity as required in interaction control algorithms. The rest of this paper is organized as follows. In Section 2, the robot manipulator that is studied is introduced. The identification of dynamic parameters is presented in Section 3. Simultaneous estimation of velocity and external force is proposed in Section 4. In Section 5, two existing algorithms for interaction force estimation are introduced and compared with the developed approach. Concluding remarks are given at the end of the paper.

2 Problem Formulation

The platform under study is a four-degree-of-freedom commercial robot manipulator (Whole Arm Manipulator, or WAM) as shown in Fig. 1. The first and the third joints are fixed in order to simplify the system into a planar two-link manipulator.

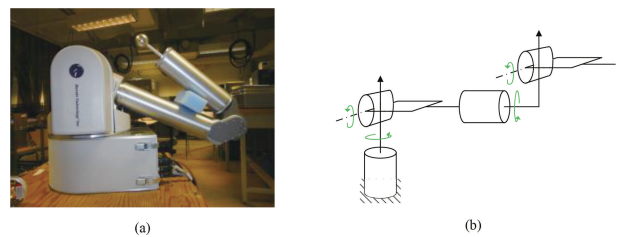


Fig. 1 (a) WAM; (b) Schematic representation of WAM.

A schematic representation of the simplified two-link robot is shown in Fig. 2.

The robot manipulator is equipped with joint position encoders. However, there are no joint tachometers and force sensor to sense the joint velocities and the interaction force.

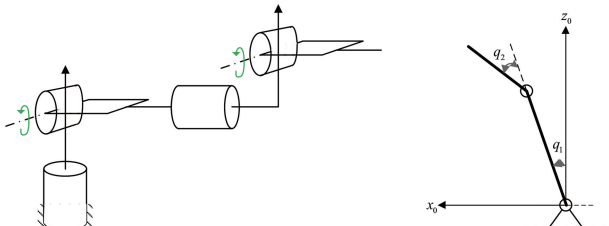


Fig. 2 Schematic representation and coordinate frame of simplified two-link WAM.

In order to study the effectiveness of the interaction force estimation algorithms, a proper motion trajectory has to be used. The Cartesian space reference trajectory that is used in the present work is shown in Fig. 3. The corresponding joint space reference trajectory is shown in Fig. 4. The reference trajectory is selected so that the manipulator will not pass through the singularity positions (or for joint 2) of the manipulator. Hence, the robust singularity handling algorithm is not used in the control algorithms.

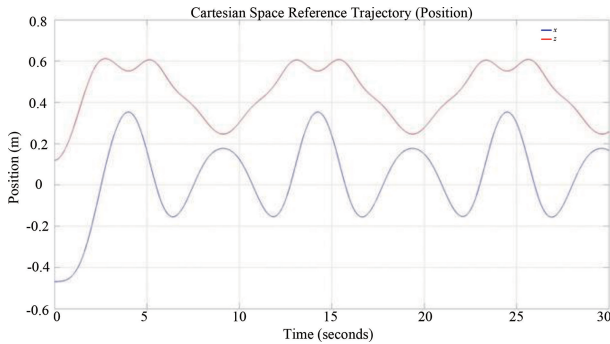


Fig. 3 Cartesian space reference trajectory in validation experiment.

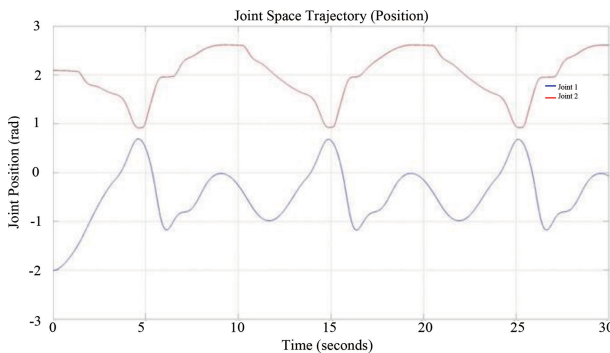


Fig. 4 Joint space reference trajectory in validation experiment.

When the trajectory tracking controllers are implemented, the robot end-effector will interact with the environment. A force sensor is placed at the end-effector to measure the interaction force. This force sensor is used for validation purposes only. The experimental setup for calibration is shown in Fig. 5.



Fig. 5 Experimental setup for validation of the interaction force estimation algorithm.

The coordinate system of the force sensor as defined by the manufacturer in software is shown in Fig. 6. Data logging of the force sensor is done using a separate interface in the host PC, which runs Microsoft Windows.

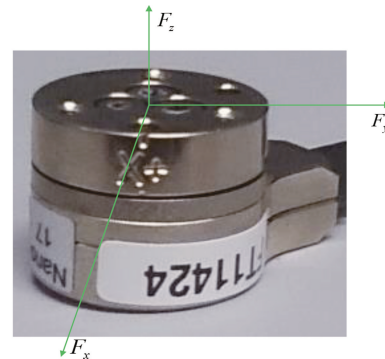


Fig. 6 Coordinate system of the force sensor.

The validation scheme is indicated in Fig. 7. Here the trajectory tracking algorithms that use joint space inverse dynamics will be employed. The observed interaction force and the measured interaction force will be compared to verify the effectiveness of the interaction force estimation algorithms.

Ideally, if the joint encoder readings are free of measurement noise, the velocity information can be reconstructed by direct differentiation. If the dynam-

ics model of the robot manipulator is precise, the external interaction force can be determined explicitly from the dynamics model of the robot manipulator in constrained motion. However, the dynamic parameters provided by the robot manufacturer are not accurate. Also, there is significant measurement noise in the encoder. The dynamics model of the studied manipulator will be identified in the next section.

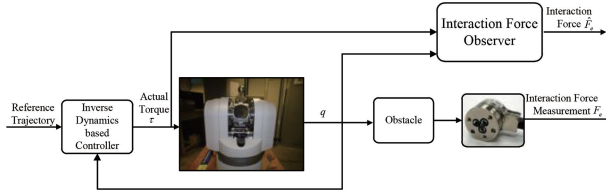


Fig. 7 The validation scheme of the interaction force estimation.

3 Dynamic Parameter Identification

The robot manufacturer provided some dynamic parameters based on a CAD model of the manipulator. However, deviations are expected in the actual dynamic parameters since some error is unavoidable during the manufacturing process. Additionally, the joint frictional torque is ignored by the manufacturer. The joint space dynamic model of the robot manipulator is given by

$$M(q)\ddot{q} + C(q, \dot{q})\dot{q} + F_v\dot{q} + F_c \text{sgn}(\dot{q}) + G(q) = \tau - J^T(q)F_e \quad (1)$$

where

q - joint position vector (2×1)

\dot{q} - joint velocity vector (2×1)

\ddot{q} - joint acceleration vector (2×1)

$M(q)$ - inertia matrix (2×2)

$C(q, \dot{q})$ - Coriolis and centrifugal matrix (2×2)

F_v - viscous friction matrix (2×2)

F_c - Coulomb friction matrix (2×2 diagonal)

$\text{sgn}(\dot{q})$ - 2×1 vector whose components are sign functions of joint velocity

$G(q)$ - gravity vector (2×1)

τ - joint actuator torque vector, (2×1)

$J(q)$ - Jacobian of the manipulator (2×2)

F_e - external interaction force (2×1)

In order to enhance the accuracy of the interaction force estimation, the dynamic parameters of the manipulator will be identified as well. An offline dynamic parameter identification algorithm could be used to obtain the dynamic parameters. However, due to the uncertainty of the friction parameter in each joint, the identified model could not accurately characterize the dynamics of the manipulator. Neural network-based compensator shown in Fig. 8 is used to handle this uncertainty.

A neural network with one hidden layer and back propagation algorithm is used here. Since the calculation of the joint torque residue is based on the states of the two joints, the compensation torques for joint 1 and joint 2 are considered simultaneously using the same neural network shown in Fig. 8.

Eight hidden layer nodes are used. Also, w_{ij} = connection weight between the input layer and the hidden layer; w_{jk} = connection weight between the hidden layer and the output layer; $\Delta\tau_1$ = torque compensation for joint 1; and $\Delta\tau_2$ = torque compensation for joint 2.

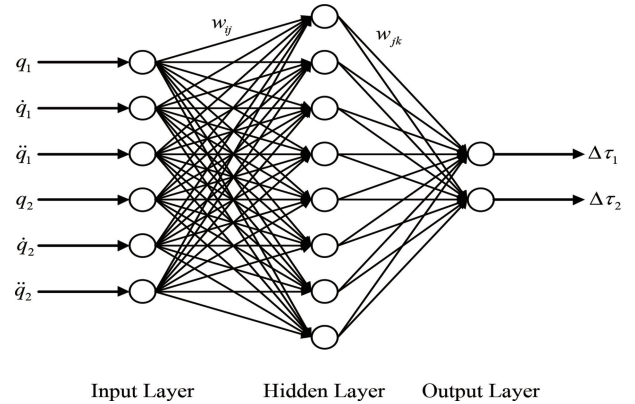


Fig. 8 Neural Network based torque compensator.

As the activation function, the sigmoid function is used here as given by

$$\sigma(x) = \frac{1}{1 + e^{-x}} \quad (2)$$

The inputs to the neural network are the joint states, which are given by the corresponding joint position q and joint velocity \dot{q} . In addition, joint ac-

celeration \ddot{q} is used as an input to the neural network. The velocities and accelerations are reconstructed using the sliding mode-based robust differentiator^[23]. The output of the neural network is the torque difference between the actual joint torques that are calculated using the joint actuator current, and the predicted joint torques. The neural network is trained using input data and the corresponding outputs. After training, the neural network will act as a compensator to compensate for the torque difference that will be used in the interaction force estimation algorithms.

The effectiveness of this torque compensator is studied by using the validation scheme shown in Fig. 9.

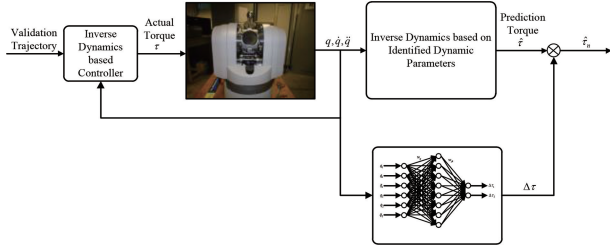


Fig. 9 Validation process of offline dynamic parameters with neural network-based compensator.

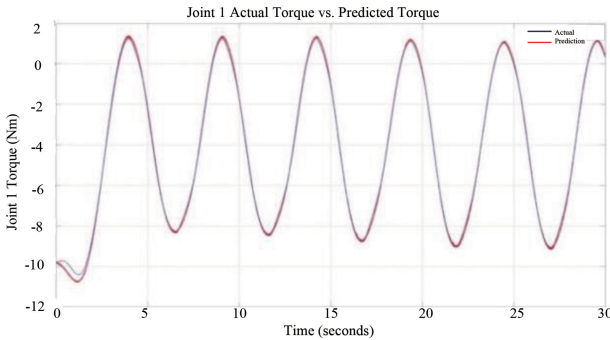


Fig. 10 Joint 1 actual torque versus predicted torque.

The actual applied joint torque and the predicted torque are compared and the results are shown in Fig. 10-Fig. 13. It is observed from these results that the dynamic model is sufficiently accurate when integrating the neural network-based compensator in the validation process. The identified dynamic parameters and the compensator are used in the interaction force estimation algorithm given in the next section.

tion.

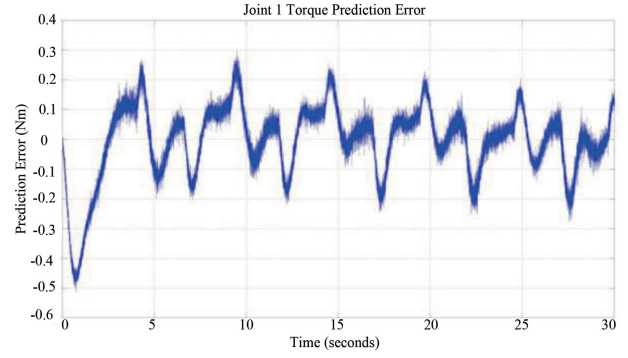


Fig. 11 Joint 1 torque prediction error.

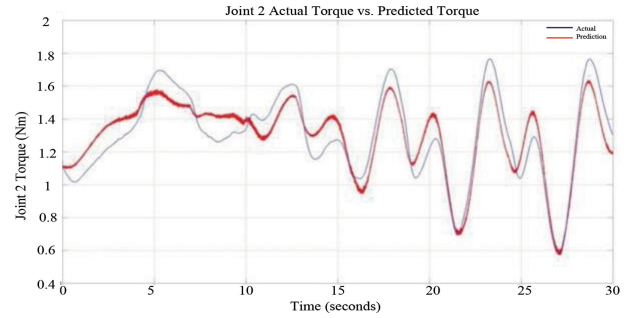


Fig. 12 Joint 2 actual torque versus predicted torque.

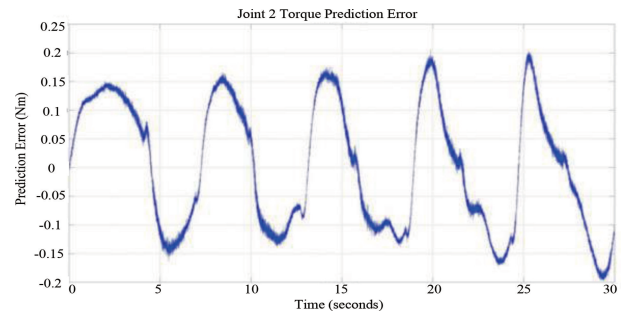


Fig. 13 Joint 2 torque prediction error.

4 Interaction Force Estimation through Adaptive High Order Sliding Mode Observer

An interaction force estimation algorithm that uses an adaptive high order sliding mode observer is proposed in this section. It will facilitate robust interaction force estimation in the presence of measurement noise. First, the dynamic model of the robot manipulator as given in Eq. (1) is rewritten in the state-space representation.

Let $x_1 = q$, $x_2 = \dot{q}$, $u = \tau$. Then, the joint space robot dynamics equation may be represented in the state-space formulation as, $\dot{x}_1 = x_2$

$$f(t, x_1, x_2, u) = -M^{-1}(x_1) [C(x_1, x_2)x_2 + F_v x_2 + F_c \text{sgn}(x_2) + G(x_1) - u]$$

$$\xi(t, x_1, x_2, u) = -M^{-1}(x_1) [\Delta\tau + J^T(x_1)F_e]$$

$x_1 \in R^2$ is the joint position encoder reading; $x_2 \in R^2$ is the joint velocity of the manipulator; $f(t, x_1, x_2, u) \in R^2$ represents the nominal dynamics of the mechanical system; and $\xi(t, x_1, x_2, u)$ is the combination of the model inaccuracy induced terms $\Delta\tau$ (reconstructed from the neural network-based compensator) and the external interaction force F_e . The representations of $f(t, x_1, x_2, u) \in R^2$ and $\xi(t, x_1, x_2, u)$ are given by

$$f(t, x_1, x_2, u) = \begin{bmatrix} f_1(t, x_1, x_2, u) \\ f_2(t, x_1, x_2, u) \end{bmatrix} \quad (4)$$

$$\xi(t, x_1, x_2, u) = \begin{bmatrix} \xi_1(t, x_1, x_2, u) \\ \xi_2(t, x_1, x_2, u) \end{bmatrix} \quad (5)$$

$$\dot{x}_{1i} = \hat{x}_{2i} + \hat{\lambda}_{2i} |x_{1i} - \hat{x}_{1i}|^{2/3} \text{sign}(x_{1i} - \hat{x}_{1i}) + k_{2i}(x_{1i} - \hat{x}_{1i}) \quad (6)$$

$$\dot{x}_{2i} = f_i(x_1, \hat{x}_2, u) + \hat{\lambda}_{1i} |\dot{x}_{1i} - \hat{x}_{2i}|^{1/2} \text{sign}(\dot{x}_{1i} - \hat{x}_{2i}) + k_{1i}(\dot{x}_{1i} - \hat{x}_{2i}) + \dot{z}_i \quad (7)$$

$$\dot{z}_i = \hat{\lambda}_{0i} \text{sign}(\dot{x}_{1i} - \hat{x}_{2i}) \quad (8)$$

where $\hat{\lambda}_{2i}$, $\hat{\lambda}_{1i}$ and $\hat{\lambda}_{0i}$ are gains to be determined so as to guarantee the convergence of the estimation error.

For the derivation simplicity, a matrix representation is used for the observer as follows:

$$\dot{x}_1 = \hat{x}_2 + \hat{\lambda}_2 |x_1 - \hat{x}_1|^{2/3} \text{sign}(x_1 - \hat{x}_1) + k_2(x_1 - \hat{x}_1) \quad (9)$$

$$\dot{x}_2 = f(x_1, \hat{x}_2, u) + \hat{\lambda}_1 |\dot{x}_1 - \hat{x}_2|^{1/2} \text{sign}(\dot{x}_1 - \hat{x}_2) + k_1(\dot{x}_1 - \hat{x}_2) + \dot{z} \quad (10)$$

$$\dot{z} = \hat{\lambda}_0 \text{sign}(\dot{x}_1 - \hat{x}_2) \quad (11)$$

The variables in Eq. (9) - Eq. (11) are the vectors that correspond to the scalars of Eq. (6) - Eq. (8), as for example, used in^[22]. Before deriving the adaptation law, two new variables are defined as

$$s_2 = x_1 - \hat{x}_1 \quad (12)$$

$$\dot{x}_2 = f(t, x_1, x_2, u) + \xi(t, x_1, x_2, u) \quad (3)$$

$$y = x_1$$

where

The non-adaptive high order sliding mode observer has been implemented^[22] to reconstruct the external disturbance. A main limitation of this algorithm is that it is rather difficult to determine the observer gains to guarantee the convergence of the observer. Adaptive sliding mode based differentiators have been proposed^[21, 23]. The observer gains could be tuned on line to guarantee the convergence of the robust differentiator.

Inspired by the work^[21, 23], an adaptive sliding mode observer is designed now to reconstruct the interaction force. The observer adaption laws are designed based on the Lyapunov approach. The observer equations are

$$s_1 = \dot{x}_1 - \hat{x}_2 \quad (13)$$

The parameter λ_2^* is incorporated such that

$$\dot{q} = \dot{x}_1 = \dot{x}_2 + \lambda_2^* |x_1 - \hat{x}_1|^{2/3} \text{sign}(x_1 - \hat{x}_1) \quad (14)$$

Comparing Eq. (9) with Eq. (14), the derivative of s_2 is given by

$$\dot{s}_2 = \dot{x}_1 - \dot{\hat{x}}_1 = -(\hat{\lambda}_2 - \lambda_2^*) |s_2|^{2/3} \text{sign}(s_2) - k_2 s_2 \quad (15)$$

Let $\bar{\lambda}_2 = \hat{\lambda}_2 - \lambda_2^*$ and define the Lyapunov function V_2 :

$$V_2 = \frac{1}{2}(s_2^2 + \bar{\lambda}_2^2) \quad (16)$$

The time derivative of V_2 along the system trajectory is

$$\begin{aligned} \dot{V}_2 &= s_2 \dot{s}_2 + \bar{\lambda}_2 \dot{\bar{\lambda}}_2 \\ &= s_2 [-\bar{\lambda}_2 |s_2|^{2/3} \text{sign}(s_2) - k_2 s_2] + \bar{\lambda}_2 \dot{\bar{\lambda}}_2 \\ &= -k_2 s_2^2 + \bar{\lambda}_2 [\dot{\bar{\lambda}}_2 - s_2 |s_2|^{2/3} \text{sign}(s_2)] \end{aligned} \quad (17)$$

Select the adaption law for $\hat{\lambda}_2$ as

$$\dot{\lambda}_2 = s_2 |s_2|^{2/3} \text{sign}(s_2) \quad (18)$$

Then we have,

$$\dot{V}_2 = -k_2 s_2^2 \quad (19)$$

In this manner the convergence of s_2 is established. Similarly, the derivative of s_1 may be represented as

$$\dot{s}_1 = \hat{\dot{x}}_1 - \dot{x}_2 \quad (20)$$

There should be a parameter λ_1^* such that

$$\begin{aligned} \ddot{q} = \hat{\dot{x}}_1 = f(x_1, \hat{x}_2, u) + \\ \lambda_1^* |s_1|^{1/2} \text{sign}(s_1) + \lambda_0^* \int_0^t \text{sign}(s_1) dt \end{aligned} \quad (21)$$

By comparing Eq. (10) with Eq. (13), we have

$$\begin{aligned} \dot{s}_1 = \hat{\dot{x}}_1 - \dot{x}_2 = \\ (\lambda_1^* - \hat{\lambda}_1) |s_1|^{1/2} \text{sign}(s_1) + \\ (\lambda_0^* - \hat{\lambda}_0) \int_0^t \text{sign}(s_1) dt - k_1 s_1 \end{aligned} \quad (22)$$

Defining $\bar{\lambda}_1 = \lambda_1^* - \hat{\lambda}_1$ and $\bar{\lambda}_0 = \lambda_0^* - \hat{\lambda}_0$, we have

$$\dot{s}_1 = -\bar{\lambda}_1 |s_1|^{1/2} \text{sign}(s_1) - \bar{\lambda}_0 \int_0^t \text{sign}(s_1) dt - k_1 s_1 \quad (23)$$

A new Lyapunov function V_1 is chosen as

$$V_1 = \frac{1}{2}(s_1^2 + \bar{\lambda}_1^2 + \bar{\lambda}_0^2) \quad (24)$$

The derivative of V_1 along the system profile is given by

$$\begin{aligned} \dot{V}_1 = s_1 \dot{s}_1 + \bar{\lambda}_1 \dot{\lambda}_1 + \bar{\lambda}_0 \dot{\lambda}_0 = \\ s_1 \left[-\bar{\lambda}_1 |s_1|^{1/2} \text{sign}(s_1) - \bar{\lambda}_0 \int_0^t \text{sign}(s_1) dt - k_1 s_1 \right] + \\ \bar{\lambda}_1 \dot{\lambda}_1 + \bar{\lambda}_0 \dot{\lambda}_0 = \\ -k_1 s_1^2 + \bar{\lambda}_1 [\dot{\lambda}_1 - s_1 |s_1|^{1/2} \text{sign}(s_1)] + \\ \bar{\lambda}_0 \left[\dot{\lambda}_0 - s_1 \int_0^t \text{sign}(s_1) dt \right] \end{aligned} \quad (25)$$

Selecting the adaption law for $\hat{\lambda}_1$ and $\hat{\lambda}_0$ as

$$\dot{\lambda}_1 = s_1 |s_1|^{1/2} \text{sign}(s_1) \quad (26)$$

$$\dot{\lambda}_0 = s_1 \int_0^t \text{sign}(s_1) dt \quad (27)$$

we have

$$\dot{V}_1 = -k_1 s_1^2 \quad (28)$$

Thus, the convergence of s_1 is established. The results of the interaction force estimation are given in Fig. 14 - Fig. 17.

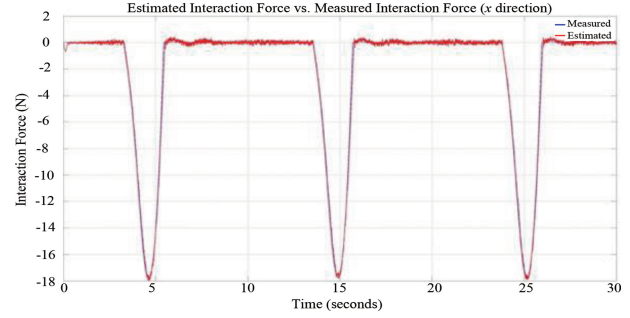


Fig. 14 Estimated force versus measured force (x direction).

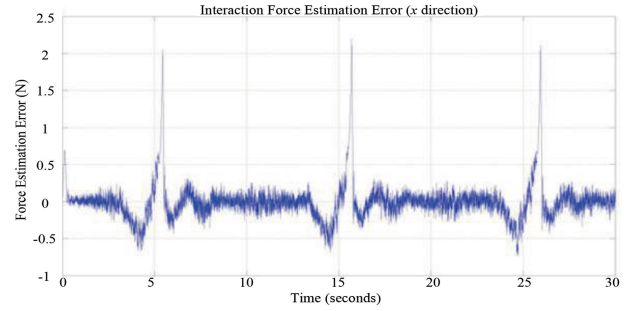


Fig. 15 Force estimation error (x direction).

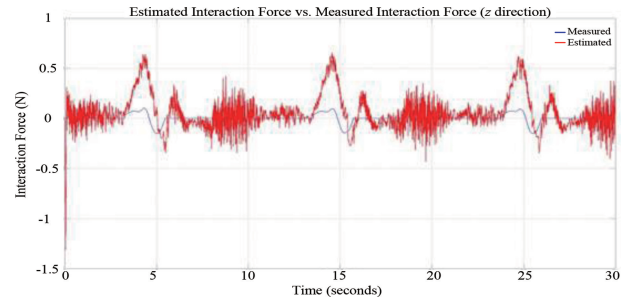


Fig. 16 Estimated force versus measured force (z direction).

It is seen that in the x direction, the interaction force reconstruction result is satisfactory. The force reconstruction error for this direction is small. However, in the z direction, the force reconstruction results are rather deteriorated. The possible cause for

this error is the sliding motion in this direction. Accordingly, when the end-effector is moving in this direction, chattering may happen.

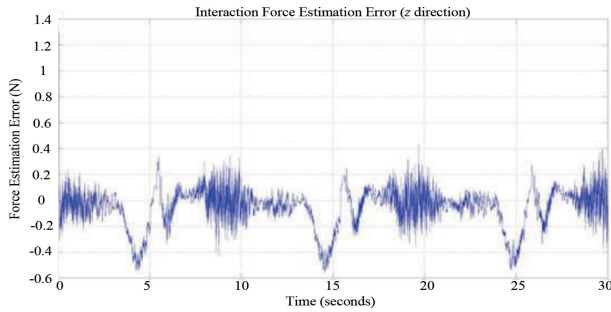


Fig. 17 Force estimation error (z direction).

5 Comparison with Other Estimation Algorithms

The interaction force observer that uses an adaptive sliding mode technique is now compared with two existing algorithms to show its superiority. The first existing method reconstructs the interaction force using inverse dynamics, while the other one uses a second order sliding mode observer for interaction force reconstruction.

5.1 Interaction Force Computation Using Identified Dynamic Model

The external interaction force can be reconstructed using the torques applied to the joint actuators and the corresponding joint motion. To improve the force estimation accuracy, the neural network-based dynamic model compensator that was presented in Section 3 is used here.

$$\hat{F}_e = J^{-T}(q) \left\{ \begin{array}{l} \tau - \Delta\tau - [\hat{M}(q)\ddot{q} + \hat{C}(q, \dot{q})\dot{q}] \\ + \hat{F}_v\dot{q} + \hat{F}_c \text{sgn}(\dot{q}) + \hat{G}(q) \end{array} \right\} \dots \quad (29)$$

Robust sliding mode-based differentiator^[23] will be used in Eq. (29) to calculate joint velocity and acceleration. The results of the interaction force reconstruction are given in Fig. 18 -Fig. 21. It may be concluded from these results that this interaction force reconstruction algorithm is inferior to the adaptive sliding mode observer as given in Section 4, with regard to the accuracy of the interaction force

estimation.

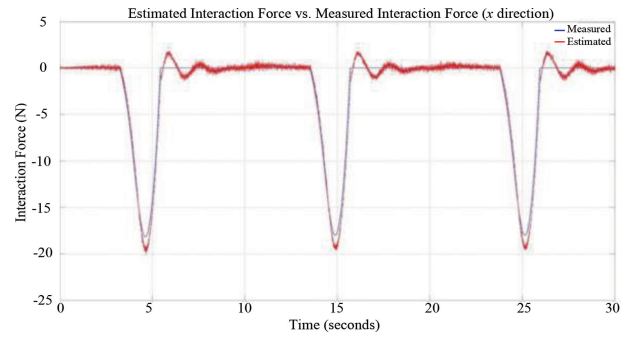


Fig. 18 Estimated force versus measured force (x direction).

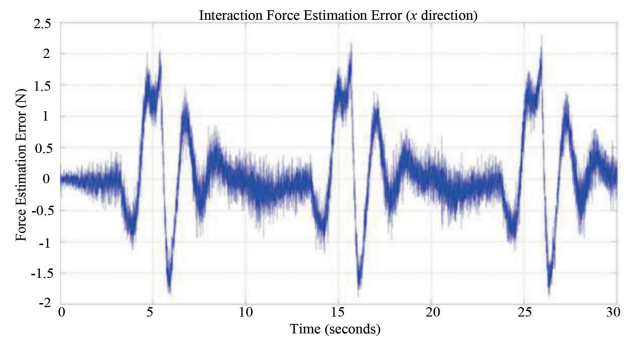


Fig. 19 Force estimation error (x direction).

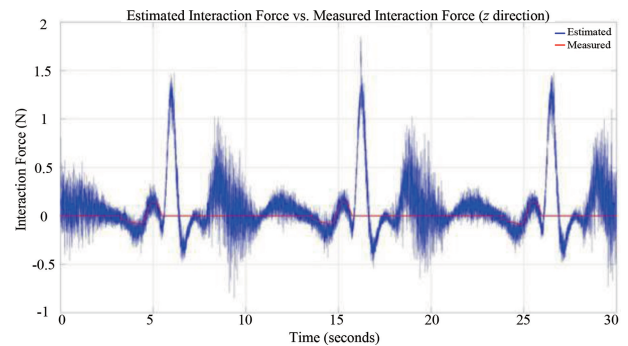


Fig. 20 Estimated force versus measured force (z direction).

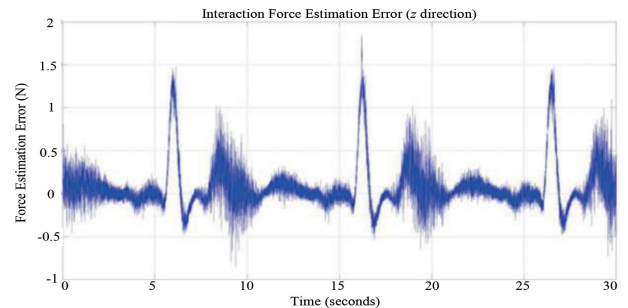


Fig. 21 Force estimation error (z direction).

5.2 Interaction Force Estimation Using 2nd Order Sliding Mode Observer

Observation of the states and unknown inputs using a second-order sliding mode observers has been studied by others. In a recent work^[24], the algorithms for state observation and unknown input reconstruction have been extended to the multi-DOF case. The same state-space model as in Section 4 will be used now for evaluating this existing method. The observer for simultaneous state and unknown input is given by

$$\dot{\hat{x}}_1 = \hat{x}_2 + z_1 \quad (30)$$

$$\dot{\hat{x}}_2 = f(t, x_1, \hat{x}_2, u) + z_2 \quad (31)$$

with $\hat{x}_1 \in R^2$, $\hat{x}_2 \in R^2$.

The i -th components ($i = 1, 2$) of z_1 and z_2 are defined as

$$z_{1i} = \lambda_i \cdot |x_{1i} - \hat{x}_{1i}|^{1/2} \cdot \text{sign}(x_{1i} - \hat{x}_{1i}) \quad (32)$$

$$z_{2i} = \alpha_i \cdot \text{sign}(x_{1i} - \hat{x}_{1i}) \quad (33)$$

The interaction force is reconstructed by passing the equivalent output feedback through the low-pass filter

$$F(s) = \frac{1}{T_i s + 1} \quad (34)$$

where T_i is the time constant for each variable, and is a tuning parameter. There is a tradeoff between the smoothness and the time lag of the reconstructed interaction force signal. This is illustrated by comparing the corresponding figures with different time constant. Fig. 22-Fig. 25 are the corresponding results for $T_i = 0.01$.

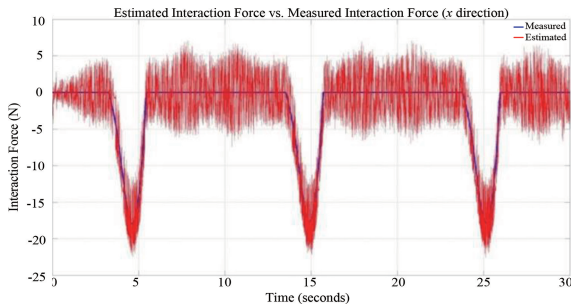


Fig. 22 Estimated force versus measured force (x direction, $T_i = 0.01$).

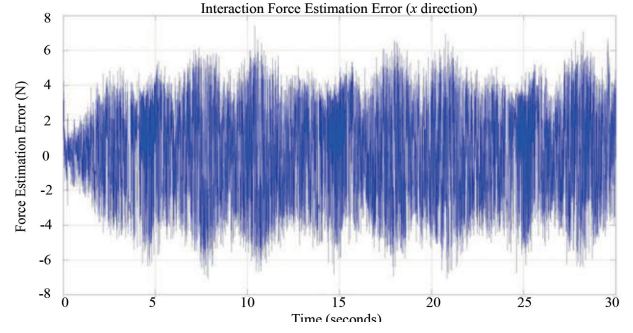


Fig. 23 Force estimation error (x direction, $T_i = 0.01$).

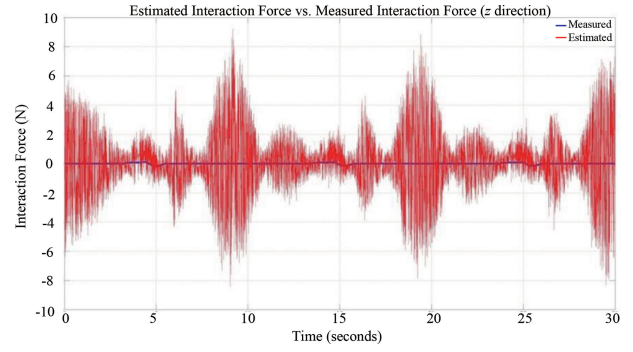


Fig. 24 Estimated force versus measured force (z direction, $T_i = 0.01$).

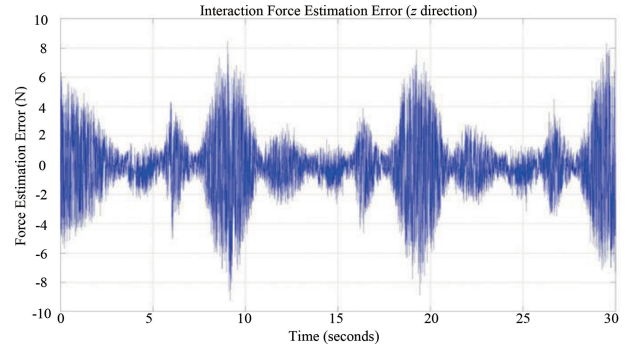


Fig. 25 Force estimation error (z direction, $T_i = 0.01$).

Fig. 31. Fig. 26 - Fig. 29 are the results for $T_i = 0.1$. It is seen that the reconstructed interaction force is smoother when compared with the corresponding results for $T_i = 0.01$. However, the delay between the estimated signal and the measured one is much larger. This presents a trade-off as mentioned before. $T_i = 0.05$ is selected and the corresponding experimental results are given in

Fig. 30 - Fig. 33. It is observed that the smoothness of the force reconstruction results and the time lag are between the corresponding results for $T_i = 0.1$ and $T_i = 0.01$. This trade-off is unavoidable due to the presence of the low-pass filter. The adaptive high-order sliding mode observer that was proposed in Section 4 does not need a low-pass filter and reconstructs the interaction force directly.



Fig. 26 Estimated force versus measured force (x direction, $T_i = 0.1$).

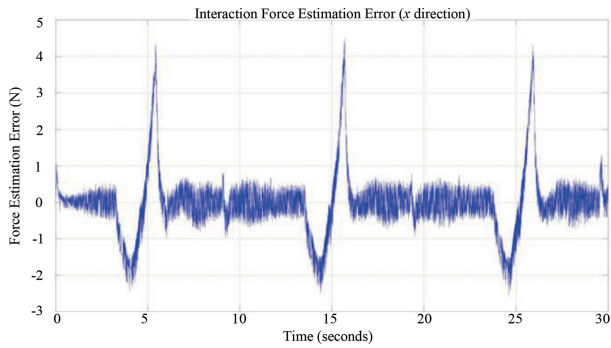


Fig. 27 Force estimation error (x direction, $T_i = 0.1$).

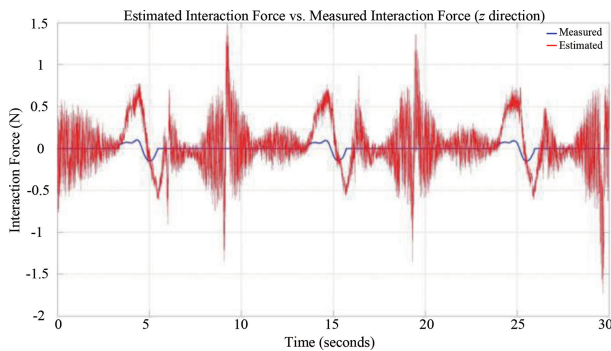


Fig. 28 Estimated force versus measured force (z direction, $T_i = 0.1$).

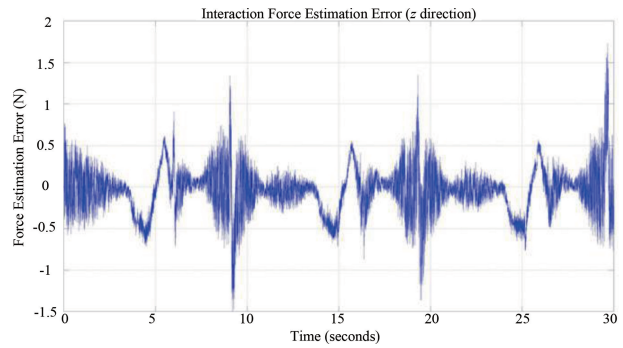


Fig. 29 Force estimation error (z direction, $T_i = 0.1$).

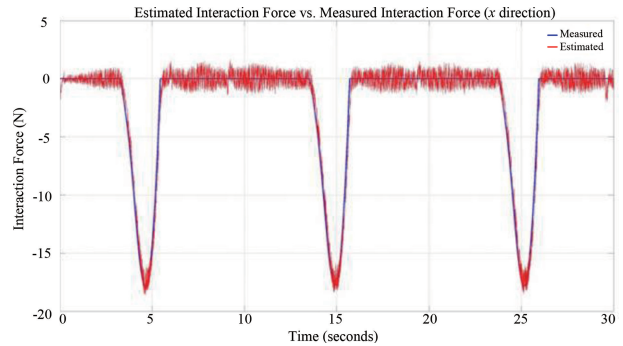


Fig. 30 Estimated force versus measured force (x direction, $T_i = 0.05$).

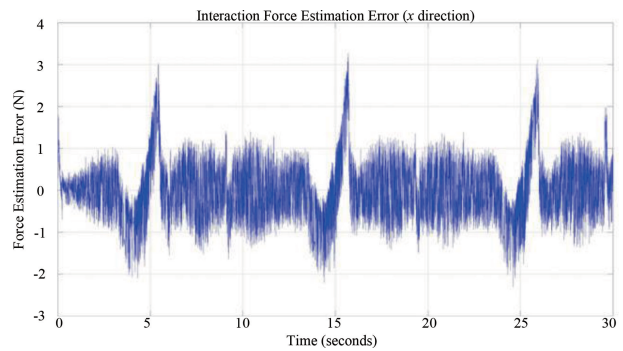


Fig. 31 Force estimation error (x direction, $T_i = 0.05$).

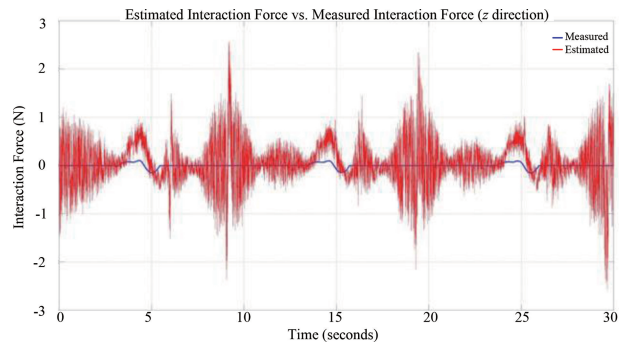


Fig. 32 Estimated force versus measured force (z direction, $T_i = 0.05$).

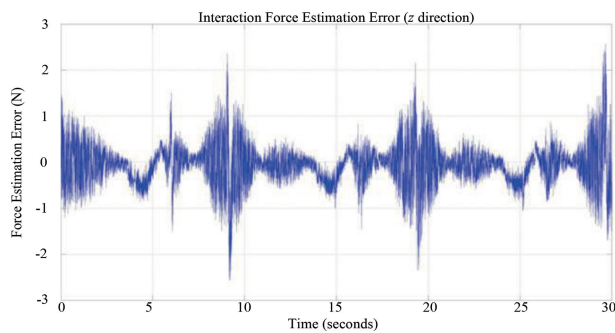


Fig. 33 Force estimation error (z direction, $T_i = 0.05$).

6 Conclusion

In this paper, an algorithm for interaction force estimation, which employed adaptive high-order sliding mode observer was proposed. It was able to estimate the interaction force effectively without the knowledge of the uncertainty bound. In order to enhance the accuracy of interaction force estimation, a dynamic model was identified for the studied manipulator. A neural network-based compensator was applied to represent the uncertainty in joint friction. The effectiveness of the developed algorithm was verified by experiments. The advantage of the proposed algorithm over two existing methods was demonstrated through experiments.

References

- [1] Whitney, D. E., (1987). Historical perspective and state of the art in robot force control. *The International Journal of Robotics Research*, 6(1), pp.3-14.
- [2] Chiaverini, S., Siciliano, B., and Villani, L., (1999). A survey of robot interaction control schemes with experimental comparison. *IEEE/ASME Transactions on Mechatronics*, 4(3), pp.273-285.
- [3] Garca, J.G., Robertsson, A., Ortega, J.G., and Johansson, R., (2008). Sensor fusion for compliant robot motion control. *IEEE Transactions on Robotics*, 24(2), pp.430-441.
- [4] Kumar, M. and Garg, D.P., (2004). Sensor-based estimation and control of forces and moments in multiple cooperative robots. *Journal of Dynamic Systems, Measurement, and Control*, 126(2), pp.276-283.
- [5] Garcia, J.G., Robertsson, A., Ortega, J.G., and Johansson, R., (2004), September. Sensor fusion of force and acceleration for robot force control. In 2004 *IEEE/RSJ International Conference on Intelligent Robots and Systems (IROS) (IEEE Cat. No. 04CH37566)* (Vol. 3, pp. 3009-3014). IEEE.
- [6] Ohnishi, K., Shibata, M., and Murakami, T., (1996). Motion control for advanced mechatronics. *IEEE/ASME Transactions on Mechatronics*, 1(1), pp.56-67.
- [7] Mitsantisuk, C., Ohishi, K., and Katsura, S., (2012). Estimation of action/reaction forces for the bilateral control using Kalman filter. *IEEE Transactions on Industrial Electronics*, 59(11), pp.4383-4393.
- [8] Katsura, S., Matsumoto, Y., and Ohnishi, K., (2006). Analysis and experimental validation of force bandwidth for force control. *IEEE Transactions on Industrial Electronics*, 53(3), pp.922-928.
- [9] Eom, K.S., Suh, I.H., Chung, W.K., and Oh, S. R., (1998), May. Disturbance observer based force control of robot manipulator without force sensor. In *Proceedings. 1998 IEEE International Conference on Robotics and Automation (Cat. No. 98CH36146)* (Vol. 4, pp. 3012-3017). IEEE.
- [10] Jeong, J. W., Chang, P. H., and Park, K. B., (2011). Sensorless and modelless estimation of external force using time delay estimation; application to impedance control. *Journal of Mechanical Science and Technology*, 25(8), p.2051.
- [11] Bhattacharjee, T., Son, H. I., and Lee, D. Y., (2008), August. Haptic control with environment force estimation for telesurgery. In 2008 *30th Annual International Conference of the IEEE Engineering in Medicine and Biology Society* (pp. 3241-3244). IEEE.
- [12] Wang, Y. and de Silva, C.W.,(2014), August. An experimental setup for dynamics control of robot manipulators. In 2014 *9th International Conference on Computer Science & Education* (pp. 123-128). IEEE.
- [13] Chen, C. Y., Cheng, M. H. M., Yang, C. F., and Chen, J. S., (2008), June. Robust adaptive control for robot manipulators with friction. In 2008 *3rd International Conference on Innovative Computing Information and Control* (pp. 422-422). IEEE.
- [14] Le Tien, L., Albu-Schaffer, A., De Luca, A., and Hirzinger, G., (2008), September. Friction observer

- and compensation for control of robots with joint torque measurement. In 2008 *IEEE/RSJ International Conference on Intelligent Robots and Systems* (pp. 3789-3795). IEEE.
- [15] Namvar, M., (2009). A class of globally convergent velocity observers for robotic manipulators. *IEEE Transactions on Automatic Control*, 54(8), pp.1956-1961.
- [16] Yih, C.C., (2012). Extended Nicosia-Tomei velocity observer-based robot-tracking control. *IET Control Theory & Applications*, 6(1), pp.51-61.
- [17] Lotfi, N. and Namvar, M., (2010), May. A globally convergent observer for velocity estimation in robotic manipulators with uncertain dynamics. In 2010 *IEEE International Conference on Robotics and Automation* (pp. 4645-4650). IEEE.
- [18] Daly, J.M. and Wang, D.W., (2010), October. Time-delayed bilateral teleoperation with force estimation for n-DOF nonlinear robot manipulators. In 2010 *IEEE/RSJ International Conference on Intelligent Robots and Systems* (pp. 3911-3918). IEEE.
- [19] Daly, J.M. and Wang, D.W., (2009). Output feedback sliding mode control in the presence of unknown disturbances. *Systems & Control Letters*, 58(3), pp. 188-193.
- [20] Drakunov, S. and Utkin, V., (1995), December. Sliding mode observers. Tutorial. In *Proceedings of 1995 34th IEEE Conference on Decision and Control* (Vol. 4, pp. 3376-3378). IEEE.
- [21] Sidhom, L., Smaoui, M., Thomasset, D., Brun, X., and Bideaux, E., (2011). Adaptive higher order sliding modes for two-dimensional derivative estimation. *IFAC Proceedings Volumes*, 44(1), pp.3063-3071.
- [22] Van, M., Kang, H.J., and Suh, Y.S., (2013). Second order sliding mode-based output feedback tracking control for uncertain robot manipulators. *International Journal of Advanced Robotic Systems*, 10(1), p.16.
- [23] Sidhom, L., Pham, M.T., Thévenoux, F., and Gautier, M., (2010), July. Identification of a robot manipulator based on an adaptive higher order sliding modes differentiator. In 2010 *IEEE/ASME International Conference on Advanced Intelligent Mechatronics* (pp. 1093-1098). IEEE.
- [24] Daly, J.M. and Wang, D.W., (2014). Time-delayed

output feedback bilateral teleoperation with force estimation for n-DOF nonlinear manipulators. *IEEE Transactions on Control Systems Technology*, 22(1), pp.299-306.

Authors' Biographies



Yanjun WANG obtained his PhD degree in the Department of Mechanical Engineering, University of British Columbia, Vancouver, Canada in 2014. He received his Master degree in Automotive Engineering from Shanghai Jiao Tong University, Shanghai, China in 2009, and his Bachelor degree in Automotive Engineering from Nanjing University of Aeronautics & Astronautics, Nanjing, Jiangsu, China in 2006. Presently he is working on compliance control of robotics in ViWiSTAR Technologies Ltd.. His research interests are in robot dynamics modelling and control, system identification, automotive powertrain system modeling, control and optimization, and soft computing. E-mail: yjwang@alumni.ubc.ca



Yunfei ZHANG received his B.S. degree in automation from Qingdao University of Science and Technology in 2006, and M.S. degree in automotive engineering from Shanghai Jiao Tong University, China, in 2010. He finished his Ph.D. degree the Department of Mechanical Engineering at the University of British Columbia, Canada in 2015. He is currently working on robotics technologies for caring elderly people, as an ambitious start up entrepreneur. His main research interests include deep reinforcement learning and control, decision making, robotics, and autonomous driving. E-mail: yunfeizhang0616@gmail.com



Shujun GAO received his B.S. degree from North University of China in 2008, and M.S. degree from Tianjin University, China, in 2010. He finished his Ph.D. degree in the Department of Mechanical Engineering at the University of British Columbia, Canada in

2017. His main research interests include deep learning, computer vision, engineering optimization.

E-mail: shujun.gao@mech.ubc.ca



Clarence W. de Silva received Ph.D. degrees from Massachusetts Institute of Technology, Cambridge, USA, in 1978, and the University of Cambridge, Cambridge, U. K., in 1998, and the Honorary D.Eng. degree from the University of Waterloo, Waterloo, ON, Canada, in 2008. He has been a Professor of Mechanical Engineering and NSERC-BC Packers Chair in Industrial Automation at the University of British Columbia, Vancouver, BC, Canada, since 1988, and also the Tier 1 Canada Research Chair in Mechatronics and Industrial Automation. He has authored 24 books and more than 550 papers, approximately half of which are in journals. His recent books

published by Taylor & Francis/CRC are: *Modeling of Dynamic Systems—with Engineering Applications* (2018); *Sensor Systems* (2017); *Sensors and Actuators—Engineering System Instrumentation, 2nd edition* (2016); *Mechanics of Materials* (2014); *Mechatronics—A Foundation Course* (2010); *Modeling and Control of Engineering Systems* (2009); *Sensors and Actuators—Control System Instrumentation* (2007); *VIBRATION—Fundamentals and Practice* (2nd ed., 2007); *Mechatronics—An Integrated Approach* (2005); and by Addison Wesley: *Soft Computing and Intelligent Systems Design—Theory, Tools, and Applications* (with F. Karray, 2004). Dr. de Silva is a Fellow of: The Institute of Electrical and Electronics Engineers (IEEE), American Society of Mechanical Engineers (ASME), the Canadian Academy of Engineering, and the Royal Society of Canada.

E-mail: desilva@mech.ubc.ca



Copyright: © 2019 by the authors. This article is licensed under a Creative Commons Attribution 4.0 International License (CC BY) license (<https://creativecommons.org/licenses/by/4.0/>).